Electron. Mater. Lett., Vol. 11, No. 4 (2015), pp. 609-613
DOI: 10.1007/s13391-015-4469-3

Enhanced Multiferroic Properties in Epitaxial Yb-Doped $BiFeO_3$ Thin Films

Yoonho Ahn,[1] Jeongdae Seo,[1] Jong Yeog Son,[1,*] and Joonkyung Jang[2,*]

[1]Department of Applied Physics and Institute of Natural Sciences, Kyung Hee University, Yongin 446-701, Korea
[2]Department of Nanoenergy Engineering, Pusan National University, Busan 609-735, Korea

(received date: 16 December 2014 / accepted date: 21 April 2015 / published date: 10 July 2015)

We report the enhanced multiferroic properties of a ytterbium (Yb)-doped $BiFeO_3$ thin film ($Bi_{0.85}Yb_{0.15}FeO_3$) deposited on a (001) $SrRuO_3$/(100) $SrTiO_3$ substrate by pulsed laser deposition. The crystal structure, surface morphology, ferroelectric domain structure, and the electrical and magnetic behavior of the epitaxial $Bi_{0.85}Yb_{0.15}FeO_3$ film, 100 nm in thickness, were investigated. The results were compared with those of an undoped $BiFeO_3$ thin film. The x-ray diffraction patterns showed that both films have tetragonal-like crystal structures. Atomic force microscopy showed that the $Bi_{0.85}Yb_{0.15}FeO_3$ and $BiFeO_3$ films have flat and clear surface steps, characteristic of a layer-by-layer growth mechanism. Furthermore, the strip-like ferroelectric domain structures were clearly observed in piezoelectric force microscopy. The $Bi_{0.85}Yb_{0.15}FeO_3$ films had significantly higher remanent polarizations of approximately 73 $\mu C/cm^2$ and lower leakage currents compared to the $BiFeO_3$ thin film. Ferromagnetic enhancement was also observed in the $Bi_{0.85}Yb_{0.15}FeO_3$ film at room temperature.

Keywords: Multiferroicity, $BiFeO_3$ thin film, Yb-doping, pulsed laser deposition, ferroelectricity, ferromagnetism

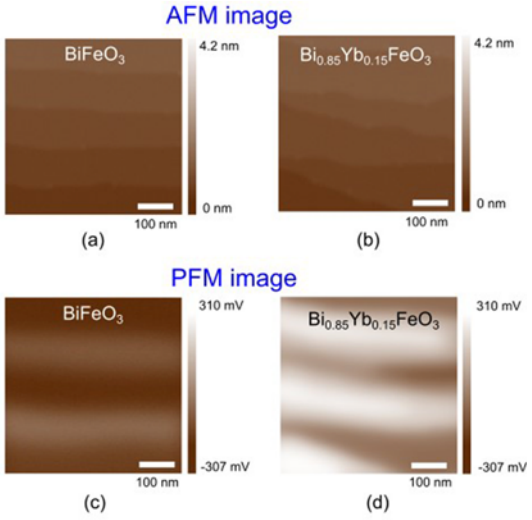

1. INTRODUCTION

Multiferroic materials, having both ferroelectric and ferromagnetic properties in the same phase, are of fundamental interest and have potential applications for magnetoelectric devices.[1-6] On the other hand, multiferroic materials generally do not possess coupling high enough to be used in magnetoelectric devices. In addition, most multiferroic materials have a low magnetic transition temperature (less than room temperature), which has limited their applications.[3,7-10]

$BiFeO_3$ has attracted considerable interest as a multiferroic material because it is lead-free and it exhibits ferroelectric and magnetic behaviors at room temperature.[11-16] Nevertheless, some critical issues of $BiFeO_3$ need to be addressed before it can be used in practical applications. That is, a high leakage current, a low ferroelectric remnant polarization, and a weak magnetization.[11,17,18] Various attempts have been made to enhance the properties of $BiFeO_3$ in device applications. The doping of $BiFeO_3$ with transition metals[18-21] or rare-earth ions[22-25] improves both the ferroelectric and ferromagnetic properties. Recently, doping of $BiFeO_3$ with Ho[26] or Ce[27] has proven to improve the ferroelectric properties of the $BiFeO_3$ films. In particular, A-site doping of $BiFeO_3$ with magnetically-active rare-earth ions is attracting significant interest as a method to overcome the aforementioned obstacles.[28-30] For example, substituting the A-site with smaller rare-earth ions resulted in tilting of the Fe^{3+}-O^{2-}-Fe^{3+} bond angles of octahedrons with a concomitant decrease in unit cell volume.[15] The Fe-O-Fe angle controls both the magnetic exchange and orbital overlap between Fe and O,[12] and is predicted to determine the electric conduction and magnetic properties.

In this study, ytterbium (Yb) was chosen as a dopant for the $BiFeO_3$ thin films because of its small atomic and ionic radii.[30] Until now, there have been few studies of Yb-doped

*Corresponding author: jyson@khu.ac.kr
*Corresponding author: jkjang@pusan.ac.kr

$BiFeO_3$ thin films. The Yb-doped $BiFeO_3$ thin film ($Bi_{0.85}Yb_{0.15}FeO_3$), which was weighed out according to its stoichiometry, was deposited on a (001) $SrRuO_3$/(100) $SrTiO_3$ substrate by pulsed laser deposition (PLD). The crystal structure, surface morphology, ferroelectric domain structure, and electrical and magnetic behavior were investigated and compared with those of undoped $BiFeO_3$ thin films. The $Bi_{0.85}Yb_{0.15}FeO_3$ thin films had a remarkably higher remanent polarization and a lower leakage current, compared to those of the $BiFeO_3$ thin film. Ferromagnetic enhancement was also observed in the $Bi_{0.85}Yb_{0.15}FeO_3$ thin film.

2. EXPERIMENTAL PROCEDURE

The PLD method was used to deposit the epitaxial $BiFeO_3$ and $Bi_{0.85}Yb_{0.15}FeO_3$ films with a thickness of 100 nm on the (001)$SrRuO_3$/(100) $SrTiO_3$ substrate. The (001) $SrRuO_3$/(100) $SrTiO_3$ substrates was prepared by depositing the $SrRuO_3$ thin film on a single crystalline (100) $SrTiO_3$ substrate (by PLD). A commercially available 1-inch $SrRuO_3$ target was used for ablation. A frequency tripled (355 nm, ~2 J/cm^2) Nd:YAG laser was used for deposition and the substrate to target distance was ~4 cm. The base pressure was ~10^{-7} Torr and an oxygen pressure of 100 mTorr was maintained before depositing the $SrRuO_3$ film. For the epitaxial deposition of the $BiFeO_3$ and $Bi_{0.85}Yb_{0.15}FeO_3$ films, 1 inch $Bi_{1.2}FeO_3$ and $BiYb_{0.15}FeO_3$ pellets were used as the PLD targets. The Bi concentration was increased to compensate for its volatilization. After the base pressure reached ~5×10^{-7} Torr, the substrate temperature was set to 800°C with an oxygen partial pressure of 100 mTorr. After deposition, the thin films were cooled to room temperature in an oxygen ambient at 300 Torr. The tentative compositions of the $BiFeO_3$ and $Bi_{0.85}Yb_{0.15}FeO_3$ thin films were confirmed by energy dispersive x-ray spectrometry.

The structures of the $BiFeO_3$ and $Bi_{0.85}Yb_{0.15}FeO_3$ thin films were examined by x-ray diffraction (XRD, CuKα radiation 1.542 Å). The thickness of the $BiFeO_3$ and $Bi_{0.85}Yb_{0.15}FeO_3$ films was 100 nm, as measured by a cross-section scanning electron microscopy. The surface morphology and ferroelectric domain structure of the $BiFeO_3$ and $Bi_{0.85}Yb_{0.15}FeO_3$ films were examined by atomic force microscopy (AFM) and piezoelectric force microscopy (PFM). Radio frequency (RF) magnetron sputtering was used to fabricate Pt top electrodes on the $BiFeO_3$ and $Bi_{0.85}Yb_{0.15}FeO_3$ films in the shape of a 100 μm wide dot with a thickness of 100 nm. These Pt top electrodes were annealed at 400°C for 5 min before obtaining the ferroelectric hysteresis loops using an RT66A (Radiant Technologies, Inc.) test system. The magnetic properties of the $BiFeO_3$ and $Bi_{0.85}Yb_{0.15}FeO_3$ thin films were analyzed from the magnetization curves under an applied magnetic field using a superconducting quantum interference device magnetometer (Quantum Design, MPMS).

3. RESULTS AND DISCUSSION

The crystal structures of the $BiFeO_3$ and $Bi_{0.85}Yb_{0.15}FeO_3$ thin films were investigated by XRD. Figure 1 presents the XRD θ-2θ patterns of the $BiFeO_3$ and $Bi_{0.85}Yb_{0.15}FeO_3$ thin films in the range, 44 - 47° 2θ. The $BiFeO_3$ and $Bi_{0.85}Yb_{0.15}FeO_3$ films showed (00l) peaks, indicating the epitaxial (00l)-oriented growth on the (001) $SrRuO_3$/(100) $SrTiO_3$ substrate. For the $Bi_{0.85}Yb_{0.15}FeO_3$ thin film, the left shift of the (002) peak from that of the $BiFeO_3$ suggests that Yb doping elongated the out-of-plane lattice axis. The full width at half maximum (FWHM) of the (002) peak of the $BiFeO_3$ and $Bi_{0.85}Yb_{0.15}FeO_3$ films were approximately 0.3° and 0.4°, respectively. The FWHMs of the rocking curves were also measured as an indicator of crystallinity. The rocking curve FWHMs of the (001) and (002) peaks were 0.5° and 0.7°, respectively, for the $BiFeO_3$ and $Bi_{0.85}Yb_{0.15}FeO_3$ thin films. This suggests that these films have good crystallinity. Owing to these highly crystallized $BiFeO_3$ and $Bi_{0.85}Yb_{0.15}FeO_3$ thin films, the lattice misfit between the thin films and (001) $SrRuO_3$ bottom electrode was as low as approximately 0.1%. From the two (002) peaks, we obtained the c-lattice constants of the $BiFeO_3$ and $Bi_{0.85}Yb_{0.15}FeO_3$ thin films as 4.00 and 4.05 Å, respectively.

The in-plane orientation was checked by performing Φ-scans of the (110) peak for the $BiFeO_3$ and $Bi_{0.85}Yb_{0.15}FeO_3$ thin films, the (111) peak for the $SrRuO_3$ bottom electrode, and the (110) peak for the (100) $SrTiO_3$ substrate. Although not shown here, the four-fold symmetries of all in-plane peaks were observed. For the $BiFeO_3$ and $Bi_{0.85}Yb_{0.15}FeO_3$ thin films, the rocking curve FWHM of the (110) peak was

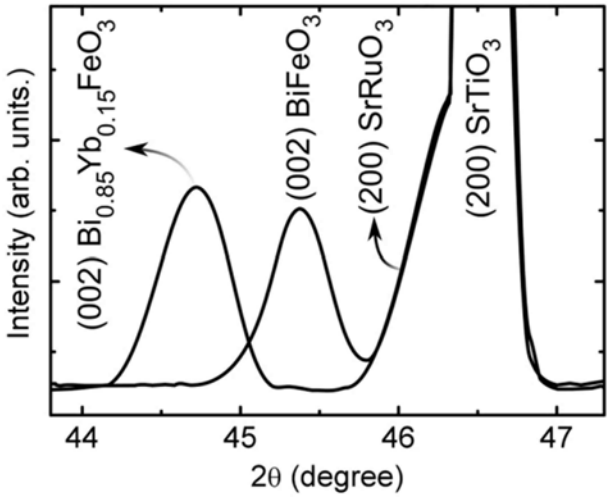

Fig. 1. XRD patterns of the epitaxial $BiFeO_3$ and $Bi_{0.85}Yb_{0.15}FeO_3$ thin films on (001) $SrRuO_3$/(100) $SrTiO_3$ substrates.

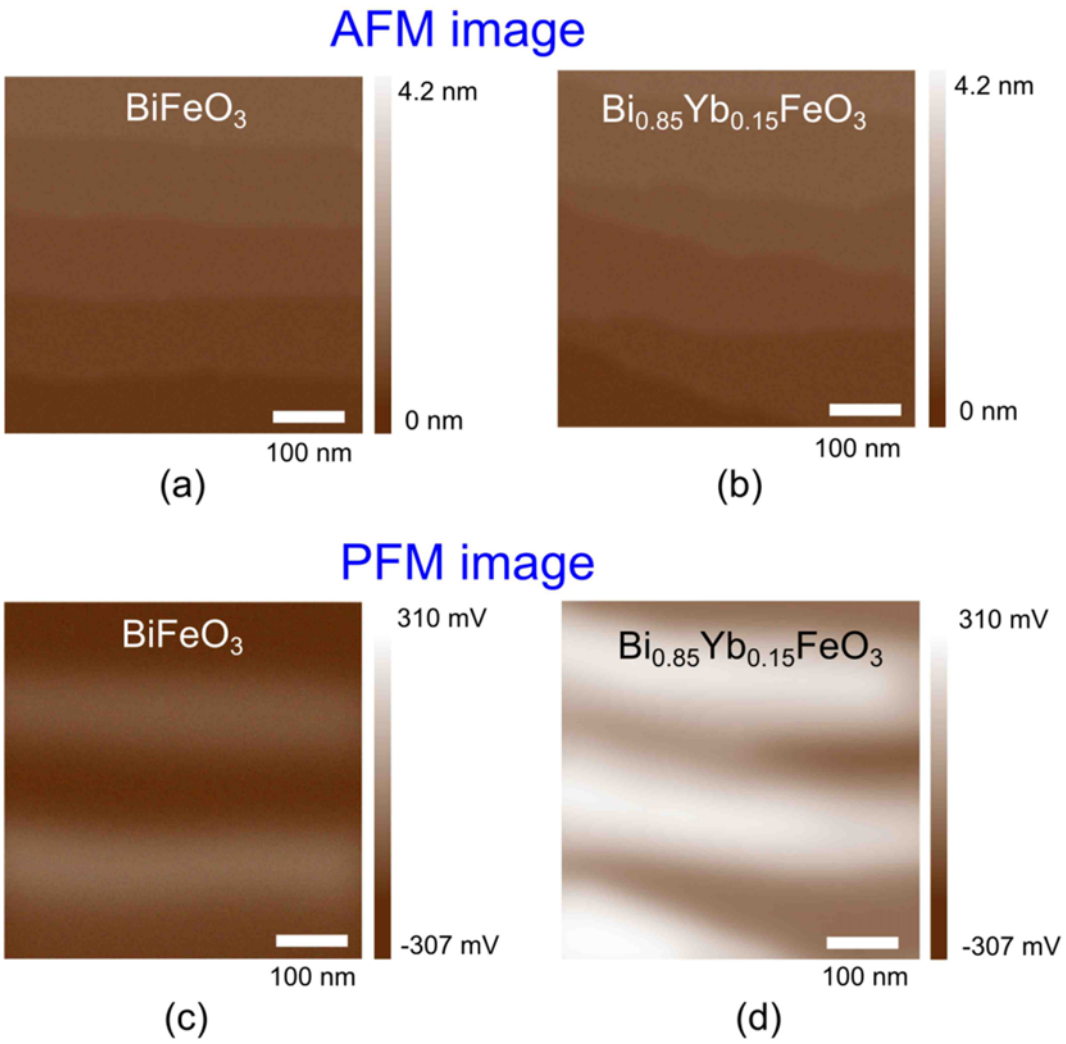

Fig. 2. AFM ((a) and (b)) and PFM ((c) and (d)) images of the $BiFeO_3$ and $Bi_{0.85}Yb_{0.15}FeO_3$ thin films.

~0.4° and 0.6°, respectively. This also indicates a well-defined structure along the in-plane orientation. From these peaks, the *a*-lattice constants for the $BiFeO_3$ and $Bi_{0.85}Yb_{0.15}FeO_3$ thin films were calculated to be 3.94 Å and 3.93 Å, respectively. Overall, the $BiFeO_3$ and $Bi_{0.85}Yb_{0.15}FeO_3$ films had a good tetragonal-like perovskite structure. The crystal structure of the bulk $BiFeO_3$ was reported to be a rhombohedrally-distorted simple cubic cell.[31] The tetragonal-like structure might arise from the strain due to the lattice mismatch between the thin film and the SRO electrode.

Figure 2 shows the AFM and PFM images of the $BiFeO_3$ and $Bi_{0.85}Yb_{0.15}FeO_3$ films. The terrace patterns in both films indicate that the films have flat and clear surface steps arising from a layer-by-layer growth mechanism (Fig. 2(a) and 2(b)). This agrees well with those previously reported for the La doping of $BiFeO_3$ films.[32] The intervals between the surface steps were roughly equal for the $BiFeO_3$ film, whereas oblique lines were observed for the $Bi_{0.85}Yb_{0.15}FeO_3$ film. The PFM images of the $BiFeO_3$ and $Bi_{0.85}Yb_{0.15}FeO_3$ films had strip-like ferroelectric domain structures, which match their AFM images (Fig. 2(c) and Fig. 2(d)). These PFM images with opposite contrast clearly reveal the distinct domains with up (bright region) and down (dark region) polarization. The ferroelectric domain structures were 100 and 130 nm in size, respectively.

The leakage current was checked by varying the applied voltage for the Pt/$BiFeO_3$/$SrRuO_3$ and Pt/$Bi_{0.85}Yb_{0.15}FeO_3$/$SrRuO_3$ capacitors (Fig. 3(a)). The leakage current of the $Bi_{0.85}Yb_{0.15}FeO_3$ film was reduced greatly by one or two orders of magnitude from that of the $BiFeO_3$ film under an applied voltage. Several mechanisms have been proposed to explain the leakage current conduction for $BiFeO_3$.[18,33-37] The present paper suggests that the reduced leakage current can be attributed to the oxygen vacancy concentration reported previously.[30] Oxygen vacancies, which are created to compensate for the positive charge deficiency caused by

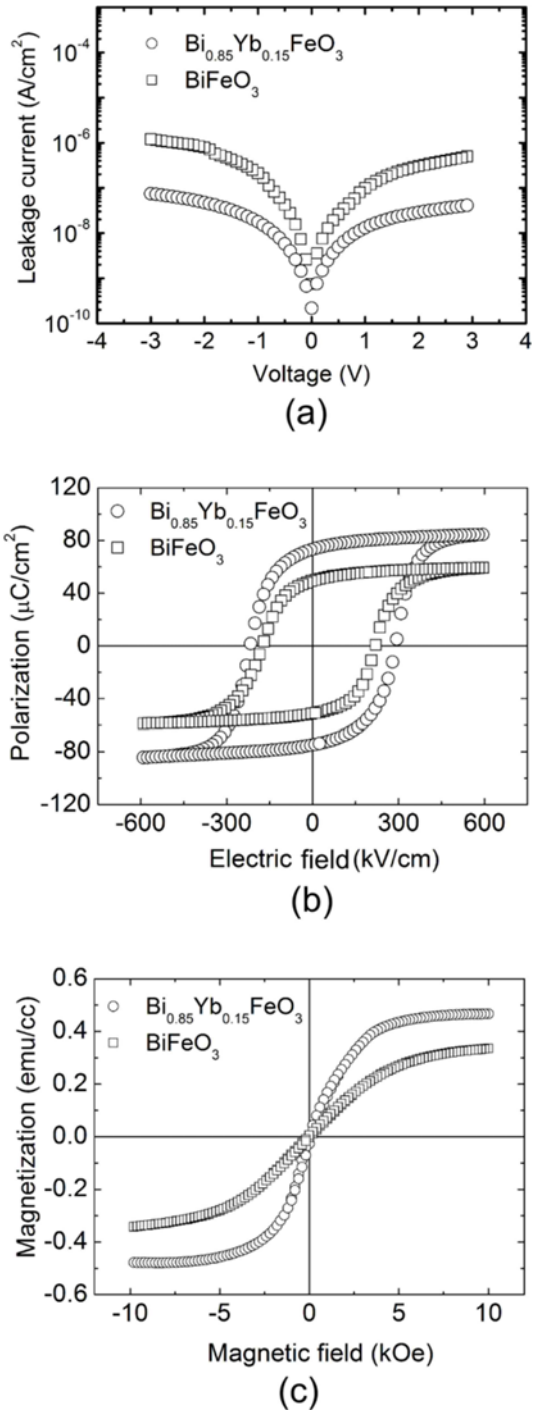

Fig. 3. (a) Leakage current vs. applied voltage for the $Pt/BiFeO_3/SrRuO_3$ and $Pt/Bi_{0.85}Yb_{0.15}FeO_3/SrRuO_3$ capacitors. (b) Hysteresis loops of the $Pt/BiFeO_3/SrRuO_3$ and $Pt/Bi_{0.85}Yb_{0.15}FeO_3/SrRuO_3$ capacitors. The remanent polarizations were 73 $\mu C/cm^2$ and 50 $\mu C/cm^2$ for the $Pt/BiFeO_3/SrRuO_3$ and $Pt/Bi_{0.85}Yb_{0.15}FeO_3/SrRuO_3$ capacitors, respectively. (c) Magnetization vs. applied magnetic field for the $BiFeO_3$ and $Bi_{0.85}Yb_{0.15}FeO_3$ thin films.

the vaporization of Bi and the reduction of Fe^{3+} ions to Fe^{2+}, act as donor-like trapping centers for electrons.[37] Therefore, the electrons can be activated easily to be free for electric conduction under an applied electric field, contributing to the higher leakage current in the $BiFeO_3$ thin film. On the other hand, the leakage current of the Yb-doped $BiFeO_3$ thin film might be reduced because of the suppressed oxygen vacancies resulting from Yb doping.[35]

The remanent polarizations of the $BiFeO_3$ and $Bi_{0.85}Yb_{0.15}FeO_3$ films were measured by constructing the hysteresis loops of the $Pt/BiFeO_3/SrRuO_3$ and $Pt/Bi_{0.85}Yb_{0.15}FeO_3/SrRuO_3$ capacitors at a measurement frequency of 10 kHz. As shown in Fig. 3(b), both films develop square-like hysteresis loops with well-saturated polarization. In particular, the $Pt/Bi_{0.85}Yb_{0.15}FeO_3/SrRuO_3$ capacitor exhibits a remanent polarization (P_r) of 73 $\mu C/cm^2$, which is remarkably higher than that of the $Pt/BiFeO_3/SrRuO_3$ capacitor, 50 $\mu C/cm^2$. These values are comparable to those of other rare-earth ions, such as La, Nd and Gd.[25,32] The hysteric behavior at various frequencies in the range of 1 KHz - 1 MHz was also examined (data not shown). The coercive electric fields increased with increasing measurement frequency. In addition, small shifts in the hysteresis loops were observed because of an imprint effect due to the asymmetric electrode configuration of the top Pt electrode and bottom $SrRuO_3$ electrode.[38] The saturation polarization (P_s) of the $BiFeO_3$ and $Bi_{0.85}Yb_{0.15}FeO_3$ thin films were 58 and 86 $\mu C/cm^2$ respectively, which are slightly larger than the remanent polarizations. This is also related to the highly crystalline structures of these thin films.

$BiFeO_3$ generally shows antiferromagnetic characteristics with a *R*3*c* structure.[31] On the other hand, the $BiFeO_3$ thin films with a *P*4*mm* structure exhibited ferromagnetic characteristic.[11] The magnetic properties of $BiFeO_3$ and $Bi_{0.85}Yb_{0.15}FeO_3$ thin films at room temperature were compared. Figure 3(c) presents the magnetization as a function of the applied magnetic field for the $BiFeO_3$ and $Bi_{0.85}Yb_{0.15}FeO_3$ thin films. Their curves exhibited ferromagnetic hysteresis behavior with a clear saturation, in which the $Bi_{0.85}Yb_{0.15}FeO_3$ film has a saturation magnetization larger than that of the $BiFeO_3$ film. This enhanced ferromagnetic properties due to Yb doping could be attributed to several factors, such a spatial homogenization of spin arrangement, a distorted spin cycloid structure, a formation of Fe^{2+} ions, and a variation in the canting angles of the Fe-O-Fe bonds, as induced by the Yb substitution.[32]

4. CONCLUSIONS

Epitaxial $BiFeO_3$ and $Bi_{0.85}Yb_{0.15}FeO_3$ thin films were fabricated on a (001) $SrRuO_3$/(100) $SrTiO_3$ substrate by pulsed laser deposition. XRD showed that the epitaxial $BiFeO_3$ and $Bi_{0.85}Yb_{0.15}FeO_3$ films, 100 nm in thickness, exhibited tetragonal-like crystal structures. The $Bi_{0.85}Yb_{0.15}FeO_3$ film showed a significantly higher remnant polarization of

approximately 73 $\mu C/cm^2$ and a lower leakage current, compared to the $BiFeO_3$ thin film. Ferromagnetic enhancement in the $Bi_{0.85}Yb_{0.15}FeO_3$ thin film was also confirmed. These findings signify the improvement in the multiferroic properties of $BiFeO_3$ thin films through Yb doping

ACKNOWLEDGEMENTS

This study was supported by the National Research Foundation Grant funded by the Korea government under contract no. 2012R1A2A2A01046451. JJ gratefully acknowledges the support by the National Research Foundation (NRF) Grant funded by the Korean Government (MSIP) (No. NRF-2014R1A4A1001690).

REFERENCES

1. N. A. Hill, *J. Phys. Chem. B* **104**, 6694 (2000).
2. H. Zheng, J. Wang, S. E. Lofland, Z. Ma, L. Mohaddes-Ardabili, T. Zhao, L. Salamanca-Riba, S. R. Shinde, S. B. Ogale, F. Bai, D. Viehland, Y. Jia, D. G. Schlom, M. Wuttig, A. Roytburd, and R. Ramesh, *Science* **303**, 661 (2004).
3. W. Eerenstein, N. D. Mathur, and J. F. Scott, *Nature* **442**, 759 (2006).
4. M. Bibes and A. Barthelemy, *Nat. Mater* **7**, 425 (2008).
5. K. F. Wang, J. M. Liu, and Z. F. Ren, *Adv. Phys.* **58**, 321 (2009).
6. J. Ma, J. Hu, Z. Li, and C.-W. Nan, *Adv. Mater.* **23**, 1062 (2011).
7. T. Kimura, S. Kawamoto, I. Yamada, M. Azuma, M. Takano, and Y. Tokura, *Phys. Rev. B* **67**, 180401 (2003).
8. Z. J. Huang, Y. Cao, Y. Y. Sun, Y. Y. Xue, and C. W. Chu, *Phys. Rev. B* **56**, 2623 (1997).
9. J. Y. Son, G. K. Bog, C. H. Kim, and J. H. Cho, *Appl. Phys. Lett.* **84**, 4971 (2004).
10. C. D. Cruz, F. Yen, B. Lorenz, Y. Q. Wang, Y. Y. Sun, M. M. Gospodinov, and C. W. Chu, *Phys. Rev. B* **71**, 060407 (2005).
11. J. Wang, J. B. Neaton, H. Zheng, V. Nagarajan, S. B. Ogale, B. Liu, D. Viehland, V. Vaithyanathan, D. G. Schlom, U. V. Waghmare, N. A. Spaldin, K. M. Rabe, M. Wuttig, and R. Ramesh, *Science* **299**, 1719 (2003).
12. G. Catalan and J. F. Scott, *Adv. Mater.* **21**, 2463 (2009).
13. Y. H. Chu, Q. He, C.-H. Yang, P. Yu, L. W. Martin, P. Shafer, and R. Ramesh, *Nano Lett.* **9**, 1726 (2009).
14. K.-T. Ko, M. H. Jung, Q. He, J. H. Lee, C. S. Woo, K. Chu, J. Seidel, B.-G. Jeon, Y. S. Oh, K. H. Kim, W.-I. Liang, H.-J. Chen, Y.-H. Chu, Y. H. Jeong, R. Ramesh, J.-H. Park, and C.-H. Yang, *Nat. Commun.* **2**, 567 (2011).
15. C.-H. Yang, D. Kan, I. Takeuchi, V. Nagarajan, and J. Seidel, *Phys. Chem. Chem. Phys.* **14**, 15953 (2012).
16. N. Siadou, I. Panagiotopoulos, N. Kourkoumelis, T. Bakas, K. Brintakis, and A. Lappas, *Adv. Mater. Sci. Eng.* **2013**, 6 (2013).
17. B. Ruette, S. Zvyagin, A. P. Pyatakov, A. Bush, J. F. Li, V. I. Belotelov, A. K. Zvezdin, and D. Viehland, *Phys. Rev. B* **69**, 064114 (2004).
18. X. Qi, J. Dho, R. Tomov, M. G. Blamire, and J. L. MacManus-Driscoll, *Appl. Phys. Lett.* **86**, 062903 (2005).
19. M. Kumar and K. L. Yadav, *J. Appl. Phys.* **100**, 074111 (2006).
20. S. K. Singh, H. Ishiwara, and K. Maruyama, *Appl. Phys. Lett.* **88**, 262908 (2006).
21. S. Pattanayak, R. N. P. Choudhary, and P. R. Das, *Electron. Matter. Lett.* **10**, 165 (2014).
22. Z. X. Cheng, X. L. Wang, S. X. Dou, H. Kimura, and K. Ozawa, *J. Appl. Phys.* **104**, 116109 (2008).
23. V. V. Lazenka, A. F. Ravinski, I. I. Makoed, J. Vanacken, G. Zhang, and V. V. Moshchalkov, *J. Appl. Phys.* **111**, 123916 (2012).
24. F. Yan, M. O. Lai, and L. Lu, *J. Phys. D: Appl. Phys.* **45**, 325001 (2012).
25. V. V. Lazenka, M. Lorenz, H. Modarresi, K. Brachwitz, P. Schwinkendorf, T. Böntgen, J. Vanacken, M. Ziese, M. Grundmann, and V. V. Moshchalkov, *J. Phys. D: Appl. Phys.* **46**, 175006 (2013).
26. Q. Yun, Y. Bai, J. Chen, W. Gao, A. Bai, and S. Zhao, *Mater. Lett.* **129**, 166 (2014).
27. A. Bai, S. Zhao, and J. Chen, *J. Nanomater.* **2014**, Article ID 509408 (2014).
28. V. R. Palkar, D. C. Kundaliya, S. K. Malik, and S. Bhattacharya, *Phys. Rev. B* **69**, 212102 (2004).
29. G. L. Yuan and O. Siu Wing, *J. Appl. Phys.* **100**, 024109 (2006).
30. H. Li, W. Yang, Z. Zhou, and H. Tian, *Electron. Mater. Lett.* **9**, 649 (2013).
31. F. Kubel and H. Schmid, *Acta Crystallogr. B* **46**, 698 (1990).
32. W. H. Kim and J. Y. Son, *Appl. Phys. Lett.* **103**, 132907 (2013).
33. K. Roy, S. Mukhopadhyay, and H. Mahmoodi-Meimand, *Proc. IEEE* **91**, 305 (2003).
34. G. W. Pabst, L. W. Martin, Y.-H. Chu, and R. Ramesh, *Appl. Phys. Lett.* **90**, 072902 (2007).
35. W. Xing, Y. Ma, Z. Ma, Y. Bai, J. Chen, and S. Zhao, *Smart Mater. Struct.* **23**, 085030 (2014).
36. G. D. Hu, S. H. Fan, C. H. Yang, and W. B. Wu, *Appl. Phys. Lett.* **92**, 192905 (2008).
37. K. Abe, N. Sakai, J. Takahashi, H. Itoh, N. Adachi, and T. Ota, *Jpn. J. Appl. Phys.* **49**, 09MB01 (2010).
38. Z. Ye, M. H. Tang, Y. C. Zhou, X. J. Zheng, C. P. Cheng, Z. S. Hu, and H. P. Hu, *Appl. Phys. Lett.* **90**, 042902 (2007).